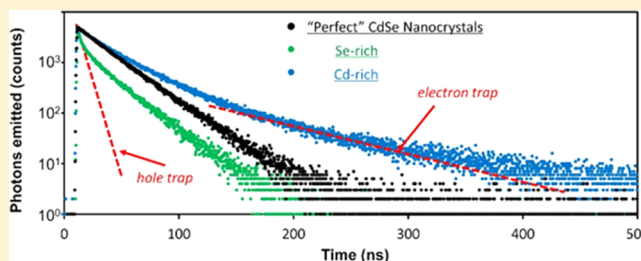


Photogenerated Excitons in Plain Core CdSe Nanocrystals with Unity Radiative Decay in Single Channel: The Effects of Surface and Ligands

Yuan Gao and Xiaogang Peng*

Center for Chemistry of Novel & High-Performance Materials, and Department of Chemistry, Zhejiang University, Hangzhou, 310027, P. R. China

ABSTRACT: A systematic and reproducible method was developed to study the decay dynamics of an exciton, a photogenerated electron–hole pair, in semiconductor nanocrystals in solution. Results revealed that the excitons in plain core CdSe nanocrystals in either zinc-blende or wurtzite or mixed lattice structures could be reproducibly prepared to decay radiatively in unity quantum yield and in single channel. The single-channel lifetime was found to increase monotonically by increasing size of the CdSe nanocrystals, with zinc-blende ones increasing in a relatively slow pace. Surface inorganic stoichiometry was found to be a sensitive parameter to affect the exciton decay dynamics for all crystal structures with different sizes. Excess Se (Cd) sites on the surface were found to induce short (long) lifetime channels for the excitons. Both types of traps reduced the quantum yield of the radiative decay of the excitons, and the hole traps associated with Se sites were nearly not emissive. With optimal surface inorganic stoichiometry, primary amines were identified as “ideal” organic ligands for CdSe core nanocrystals to achieve unity radiative decay of excitons in single channel in comparison to other types of neutral ligands commonly applied in the field.



INTRODUCTION

Synthesis of colloidal semiconductor nanocrystals in their quantum confinement size regime has gained tremendous attention in the past decades,^{1,2} because of their solution processability and size-dependent photoluminescence (PL)/electroluminescence (EL) properties. In principle, either of two emissive means is dictated by their excited state properties. Specifically, an emission process is a radiative recombination of the photo- or electro-generated electron–hole pair (exciton). Although nearly all applications as emissive materials require a semiconductor nanocrystal to be epitaxially coated with another semiconductor shell with a relatively wide band gap, it is mostly the excited states of the core that are involved with emission of light. Unfortunately, up to present, it is still challenging to synthesize core nanocrystals with ideal emissive properties, i.e., with unity radiative decay in its intrinsic channel. In fact, it is not clear whether such ideal core semiconductor nanocrystals can be achieved. We noticed that theoretical exploration on relationship between surface of semiconductor nanocrystals and their excited-state properties has started to generate some interesting insights.³ If such ideal plain core semiconductor nanocrystals indeed became available, it would be possible to correlate theoretical models with experimental observations.

For most common semiconductor nanocrystals, i.e., CdSe ones, Jasieniak et al.⁴ speculated that their emission properties should be dominated by their surface, given a well-controlled interior crystal lattice. They obtained both Cd-rich and Se-rich CdSe nanocrystals through the successive ion layer adsorption

and reaction technique⁵ (SILAR). Though the maximum PL quantum yield (QY) was only up to ~50%, they could ambiguously identify that excessive Se ions on the surface (hole traps) would diminish PL much more efficiently than excess Cd ions would do. The great efficiency of the hole traps by the anion surface centers was later confirmed for CdS⁶ and CdTe⁷ nanocrystals. In the work on CdS nanocrystals, Wei et al.⁶ further suggested that anion centers on the surface created middle-gap states, which explained the great reduction of PL QY of the CdS nanocrystals with anion surface centers. The study with CdTe nanocrystals by Omogo et al.⁷ further investigated the PL decay dynamics of the nanocrystals upon photoexcitation with various surface stoichiometry, ligands, and solvents. Though they did not obtain nanocrystals with single-channel decay, they anticorrelated nonradiative decay lifetime with average radiative decay lifetime of the excited states. Recently, Subila et al.⁸ claimed that, with the same core size and surface ligands, zinc-blende (face center cubic) CdSe nanocrystals possessed about 38% PL QY, which was significantly higher than that of the wurtzite (hexagonal) CdSe nanocrystals (4.6%). Noticeably, their observation contradicted our report in 2002,⁹ i.e., > 80% PL QY for wurtzite CdSe nanocrystals coated with similar ligands.

This work designed a method for controlling the surface stoichiometry and ligands of semiconductor nanocrystals using

Received: February 6, 2015

Published: March 18, 2015

plain core CdSe nanocrystals as the model system. The results shall demonstrate that, for well-prepared plain core semiconductor nanocrystals, different types of surface hole and electron traps can be identified by PL decay dynamics coupled with PL quantum yield measurements. With optimal surface stoichiometry and ligand passivation, photogenerated excitons were found to decay radiatively in single channel with near unity yield, supposedly the intrinsic decay channel of the excitons in plain core CdSe nanocrystals. The interior structure can affect the lifetime, but all types of commonly available crystal structures of CdSe nanocrystals can afford excitons with near unity radiative decay in single channel.

RESULTS AND DISCUSSION

Experimental Design. CdSe nanocrystals in different crystal structures were synthesized following existing protocols.^{9–11} In most cases, the surface of as-synthesized CdSe nanocrystals should be Cd-rich.¹¹ For example, the nanocrystals related to Figure 1 were zinc-blende CdSe nanocrystals

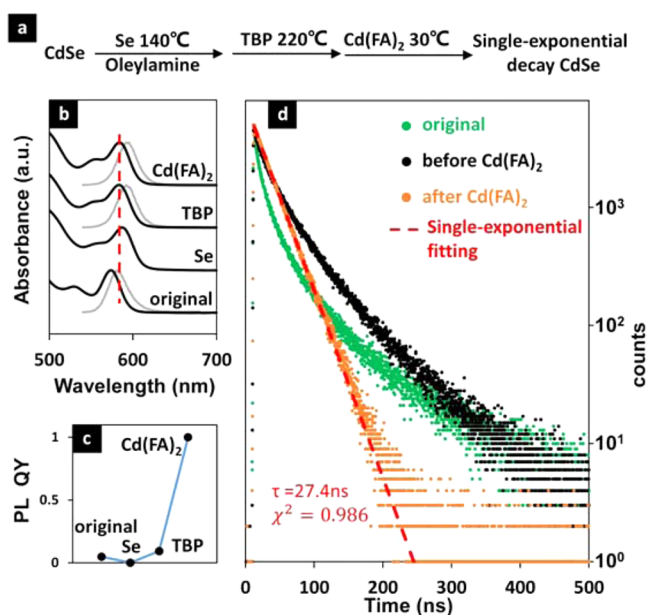


Figure 1. (a) Schematic diagram of surface stoichiometry engineering for the CdSe nanocrystals. (b) Absorbance spectra taken at different stage of surface stoichiometry engineering. (c) PL QY of CdSe nanocrystals at different stage of surface stoichiometry engineering. (d) Luminescence decay curve of CdSe nanocrystals at different stage of surface stoichiometry engineering.

synthesized in a reaction mixture with cadmium carboxylate, Se powder, fatty acid, and octadecene (ODE). These CdSe nanocrystals must be Cd-rich as the only available surface ligands in the synthetic system were carboxylate. No matter what the surface stoichiometry of the as-synthesized CdSe nanocrystal was, the first step in the chemical treatment sequence (Figure 1a) was to convert it to a Se-rich surface.

Specifically, the purified CdSe nanocrystals were mixed with oleylamine in ODE. After degassing with Ar bubbling, the mixture was heated to 140 °C, and Se powder suspended in ODE was added into the solution, which resulted in PL intensity drop. After the PL became barely detectable, more Se was added three times to ensure completed treatment. Along with the PL quenching, the UV–vis spectrum shifted to the red for a few nanometers (Figure 1b), which was consistent with

the addition of excess Se onto the surface of the original CdSe nanocrystals.⁴ In addition, necessity of fatty amine in the reaction solution to maintain colloidal stability implied that the excess surface Cd ions originally attached to carboxylate ligands were reacted with Se precursors.

After the completion of Se treatment described above, the Se-rich CdSe nanocrystals were reacted with tributylphosphine (TBP) which is a well-known passivation reagent to the Se anions on the surface of CdSe nanocrystals.^{4,12,13} Upon tributylphosphine treatment, the relative PL QY became higher than the original CdSe nanocrystals coated with carboxylate ligands (Figure 1c). However, the brightening effect of tributylphosphine was limited to a certain level; additional tributylphosphine did not further improve the situation. It should be noticed that, upon treatment with tributylphosphine, the UV–vis spectrum shifted blue slightly, presumably indicating removal of those “dangling” Se ions on the surface.

The PL QY after tributylphosphine treatment in Figure 1c was significantly lower than that observed by Jasieniak et al. (~50%).⁴ This should be a result of the complete Se treatment in this work by the use of highly reactive Se suspension in amine environment.¹⁰ Due to bulkiness of tributylphosphine, it would not be possible to passivate all Se anions on the surface of the nanocrystals in this work, resulting in relative poor emission. It should be pointed out that complete Se treatment was found to be critical for the entire treatment sequence, and the excess of Se powder in the system did not cause much trouble as long as a sufficient amount of tributylphosphine was added afterward.

Cd carboxylate should be a good option to further passivate the Se-rich surface, which might tune the surface stoichiometry at the same time. Because of the different reactivity between tributylphosphine-passivated and unpassivated Se sites, Cd carboxylate could only react with unpassivated Se sites by controlling the amount of Cd carboxylate and reaction temperature. In fact, the unpassivated Se sites were found to be so reactive that the surface reaction occurred at room temperature and changed the emission property drastically in minutes. The high reactivity of unpassivated Se sites was further evidenced by replacing Cd formate with Cd stearate, which only slightly slowed down the reaction at room temperature. Excess Cd salt would not affect the emission properties of the nanocrystals in the solution without afterward thermal annealing of the solution, which rendered the process to be controllable and reproducible.

Overall, the amounts of Se, tributylphosphine, and Cd formate needed in each step for a typical surface reaction sequence (see Experimental Section for detail) were respectively 0.04 mmol, 0.2 mL, and 5% of one monolayer of Cd atoms estimated by the stoichiometry established during epitaxial growth of CdS shell onto the CdSe nanocrystals.¹⁴ Such a small amount of Cd ions was presumably sufficient for tuning the surface stoichiometry, instead of homogeneous growth of new monolayers studied by others.^{4,6}

Completion of the entire process outlined in Figure 1a resulted in CdSe nanocrystals with nearly 100% PL QY determined by an integrating sphere. At the same time, the PL decay of the CdSe nanocrystals evolved to single-exponential decay with the best value for goodness-of-fit (χ^2) in literature, i.e., $\chi^2 = 0.986$ for the example in Figure 1d. Combination of PL QY and PL decay dynamics measurements confirmed that CdSe nanocrystals upon the treatment procedure in Figure 1a could achieve near unity radiative decay of their excited states

in single channel. In other words, the results in Figure 1 revealed that the intrinsic decay channel of the excited states of CdSe core nanocrystals could be nearly completely radiative.

Effects of Crystal Structure and Perfection of Lattice on Exciton Decay Dynamics. The process outlined in Figure 1a was applied to CdSe nanocrystals with different sizes for both zinc-blende and wurtzite structures. Figure 2a illustrates

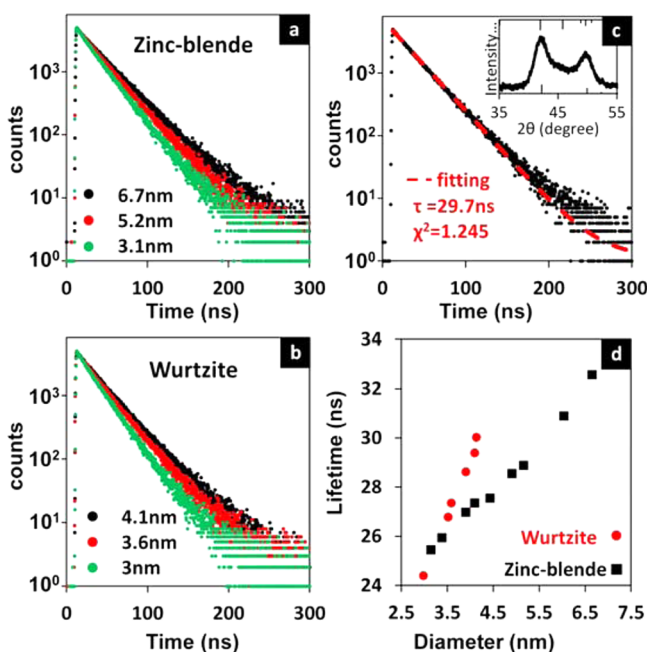


Figure 2. (a) Representative luminescence decay curve for different size of zinc-blende CdSe nanocrystals. (b) Representative luminescence decay curve for different size of wurtzite CdSe nanocrystals. (c) Luminescence decay curve of 4 nm CdSe nanocrystals with mixed lattice structure. Inset is the X-ray diffraction pattern of the sample, and the standard diffraction lines for zinc-blende CdSe (bottom) and wurtzite CdSe (top) are labeled as vertical lines. (d) Lifetime of different size CdSe nanocrystals for both wurtzite (red circle) and zinc-blende (black square) structure.

three examples of PL decay curves for zinc-blende CdSe core nanocrystals, all of which were in similar quality as the example shown in Figure 1. Specifically, single-exponential fitting for each case was excellent for measurements with high photon counts (5000), i.e., with the goodness-of-fit $\chi^2 < 1.15$. CdSe nanocrystals in zinc-blende structure smaller than ~ 3 nm in diameter were difficult to achieve single-exponential PL decay dynamics, mainly due to lack of stability during the Se treatment.

For the wurtzite structure, nanocrystals with single-exponential PL decay dynamics and near unity radiative decay of the excitons were obtained for the size range between 2.9 and 4.2 nm. We failed on the relatively large nanocrystals probably because the existence of a large portion of nonpolar facets for this structure, such as (110) and (100).¹¹ Such nonpolar facets may not be well protected by the ligand set in the current protocol. Similarly, this could also explain why single-exponential fitting for the PL decay dynamics of CdSe core nanocrystals with wurtzite structure was slightly worse ($1.2 < \chi^2 < 1.3$), though the data collected in Figure 2b did satisfy the standard, meaning $\chi^2 < 1.3$ for measurements with high photon counts.¹⁵

It is well-known that CdSe nanocrystals were often obtained with a significant amount of stacking faults along the (001) axis of wurtzite structure (equivalently, the (111) direction of zinc-blende structure).¹¹ Such nanocrystals could be readily distinguished by the X-ray powder diffraction with 2θ between 35° and 55° (X-ray wavelength being 0.154 nm) as shown in Figure 2c (inset). Result in Figure 2c illustrates that nanocrystals with such “mixed” lattice structure could also be converted to being near unity radiative decay in single channel. Interestingly, such particles usually behaved the same as perfect wurtzite CdSe core nanocrystals, with similar lifetime values and goodness-of-fit. Our early work revealed that the “mixed” structure possessed both types of facets of zinc-blende and wurtzite. It should be the poorly passivated nonpolar (110) and (100) facets from the wurtzite that made particles in the “mixed” lattice structure with wurtzite-like exciton decay dynamics. Though we could not explain similarity on lifetime values of the intrinsic PL decay channel between the pure wurtzite ones and the “mixed” lattice structure, we can conclude safely that the surface is much more important than interior for determination of emission properties of CdSe nanocrystals.

Effects of Nanocrystal Sizes on Exciton Decay Dynamics. The lifetime values for CdSe core nanocrystals with single-exponential PL decay are summarized in Figure 2d. As the size of CdSe nanocrystals increased, the intrinsic PL decay lifetime increased for both types of crystal structures. However, the single-exponential PL lifetime of zinc-blende CdSe nanocrystals increased with a relatively slow pace (Figure 2d). This could be a result of differences on the size-dependent quantum confinement¹⁶ and band-edge fine structure¹⁷ between zinc-blende and wurtzite crystals.

Theoretical^{17,18} and existing experimental^{19–21} results all indicate that the band-edge energy structure for CdSe nanocrystals is quite complex, structure sensitive, and highly size dependent. Existence of a single-channel PL decay for CdSe core nanocrystals with different sizes and crystal structures (Figure 2) implies that, at room temperature, such fine energy structures, including both bright and dark excitons, can be mixed seamlessly by thermal agitation. This means that our early explanation¹⁴ about the differences on optical quality of CdSe/CdS core/shell nanocrystals between wurtzite and zinc-blende structures was likely incorrect.

PL Decay Channels and Surface Stoichiometry. It would be difficult to delineate different decay channels from the complex PL decay dynamics of the as-synthesized CdSe nanocrystals (Figure 1b). With nanocrystals showing single PL decay channel, this problem might be solvable. Our first target was to identify the decay channels associated with Se sites on the surface.

Se suspension was added into the solution of CdSe nanocrystals with single-exponential PL decay dynamics at a temperature below 85°C . Results in Figure 3a reveal that, upon Se treatment, the UV–vis spectra did not shift noticeably. However, a small red-shift of the corresponding PL spectra (~ 2 nm in total for the example in Figure 3b) was evidenced and the PL QY dropped from $\sim 100\%$ to $\sim 5\%$ (Figure 3b). Simultaneously, some fast component(s) appeared in the PL decay dynamics curve and became more and more evident upon further addition of Se precursor (Figure 3c). Simulation yielded two short-lifetime channels in this case, i.e., ~ 2 and 12 ns, in addition to the original one at ~ 27 ns (Table 1). Appearance of fast channels usually implies appearance of

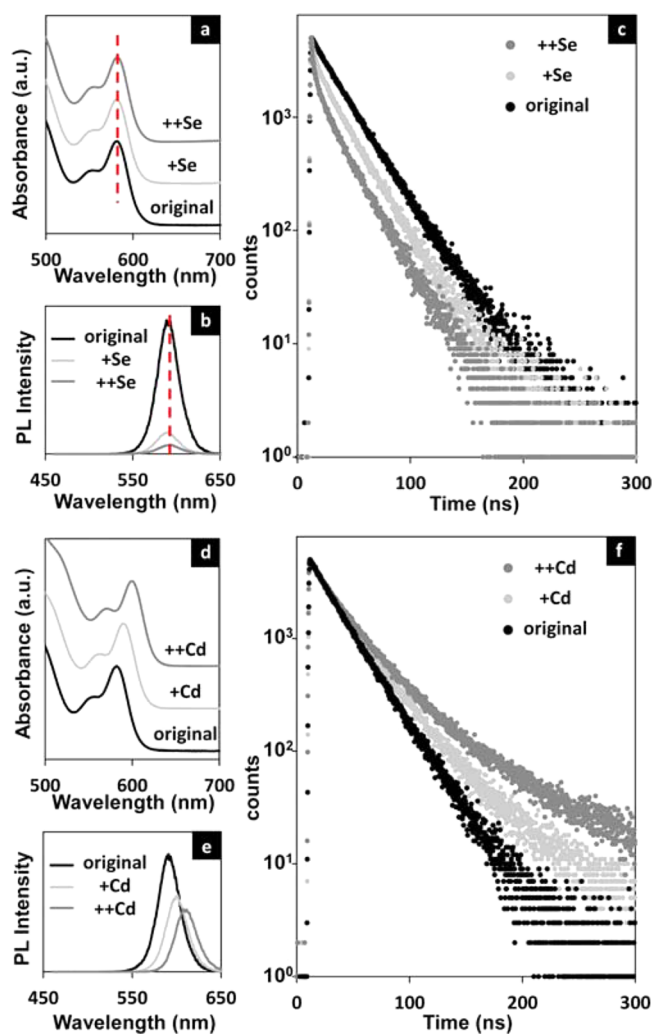


Figure 3. (a) Absorbance spectra of different stage of Se-treated CdSe nanocrystals. (b) PL spectra of different stage of Se-treated CdSe nanocrystals. (c) Luminescence decay curve of different stage of Se-treated CdSe nanocrystals. (d) Absorbance spectra of different stage of Cd-treated CdSe nanocrystals. (e) PL spectra of different stage of Cd-treated CdSe nanocrystals. (f) Luminescence decay curve of different stage of Cd-treated CdSe nanocrystals.

middle-gap states. Such middle-gap states should efficiently trap the holes and quench the PL.²²

Table 1. Lifetime and Fractional Contribution of Different Decay Channels for CdSe Nanocrystals with Different Amounts of Se Added into the Solution

	τ_1 (ns)	τ_2 (ns)	τ_3 (ns)	f_1 (%)	f_2 (%)	f_3 (%)	χ^2
original	—	—	26.8	—	—	100	1.001
+Se	2.0	12.8	26.8	2.92	18.8	78.2	1.073
++Se	1.6	11.9	26.8	7.77	29.5	62.7	0.995

Cadmium treatment was also applied to the CdSe nanocrystals with single-exponential PL decay. Excess Cd carboxylate did not affect such high quality CdSe nanocrystals with a temperature below ~ 100 °C. Upon increasing temperature to 140 °C, both UV-vis (Figure 3d) and PL (Figure 3e) spectra red-shifted with the existence of excess Cd formate in the solution. At the same time, some slow component(s) could be readily observed in the corresponding PL decay dynamics

(Figure 3f) and the PL QY dropped by $\sim 50\%$ (Figure 3e). The PL decay dynamics of the nanocrystals with excess Cd ions could be fitted with one slow channel, i.e., in the range between 55 and 75 ns, along with the original channel at ~ 26 ns for the example associated with Figures 3d–f (Table 2). These results suggested that excess Cd ions on the surface of plain core CdSe nanocrystals create shallow electron traps with relatively long lifetime.

Table 2. Lifetime and Fractional Contribution of Different Decay Channels for CdSe nanocrystals with Different Amounts of Cd Carboxylate in the Solution

	τ_1 (ns)	τ_2 (ns)	f_1 (%)	f_2 (%)	χ^2
original	26.4	—	100	—	1.002
+Cd	26.1	55.2	79.6	20.4	1.032
++Cd	26.4	70.6	67.4	32.6	1.144

Effects of Ligands on Exciton Decay Dynamics. Surface ligands should also play a role in determining the exciton decay dynamics, which is the basis of so-called electronic passivation of surface ligands. It is well-known that purification of highly emissive CdSe nanocrystals could quench the PL.^{5,9} For the CdSe core nanocrystals with single-channel PL decay, standard extraction procedure (see Experimental Section) reduced their PL QY from near unity to $\sim 65\%$ along with a noticeable red-shift of both UV-vis (Figure 4a) and PL (Figure 4b) spectra presumably by removing liable amine ligands.²³ Simultaneously, a slow component appeared in the PL decay dynamics curve (Figure 4c). Results in Figure 4a–c demonstrate that addition of amine into the nanocrystal solution after the extraction restored all optical features of the original nanocrystals before purification, including PL QY, UV-vis, and PL spectra and single-channel PL decay dynamics.

Fatty amines are electron-donating ligands and should thus passivate Cd sites on the surface. However, results in Figure 4d–f reveal that other types of common ligands, including carboxylate (Cd formate, Figure 4d), organophosphine (tributylphosphine, Figure 4e), and organophosphine oxide (trioctylphosphine oxide (TOPO), Figure 4e), could not play the same role as fatty amines. Specifically, Cd formate further diminished the PL QY, tributylphosphine showed no effects, and trioctylphosphine oxide somewhat recovered the PL QY. In all three cases, the slow component in the purified CdSe core nanocrystals more or less remained. It should be pointed out that replacement of oleylamine by other types of primary amine did not make any noticeable difference (data not shown).

CONCLUSION

To summarize, a systematic and reproducible method is introduced to study effects of surface inorganic stoichiometry and organic ligands on decay dynamics of the photogenerated excitons in CdSe nanocrystals. Results revealed that CdSe core nanocrystals can be prepared for the excitons with unity radiative decay in single channel. A delicate balance of inorganic stoichiometry, such as with/without 5% of one monolayer of Cd carboxylate, must be in place for obtaining ideal exciton decay dynamics. Such delicate balance might explain the long existing mystery of the “bright point” during the growth of CdSe core nanocrystals observed by the Weller’s group²⁴ and our group.⁹ Evidences further imply that the crystal structure, either zinc-blende or wurtzite, might not be the key to reach optimal photoluminescence properties for CdSe core nano-

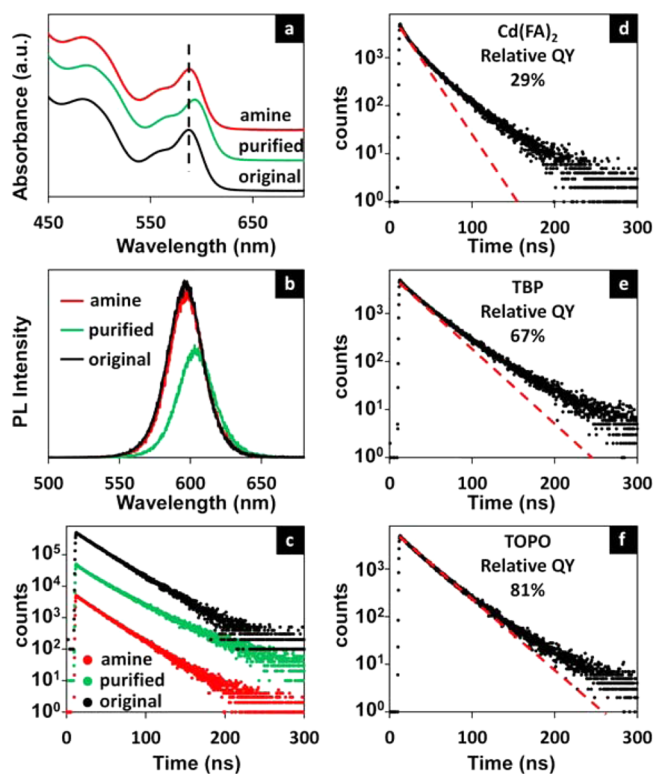


Figure 4. (a) Absorbance spectra of CdSe nanocrystals with different amine coverage. (b) PL spectra of CdSe nanocrystals with different amine coverage. (c) Luminescence decay curve of CdSe nanocrystals with different amine coverage (different decay curves were separated by a factor of 10). (d) Luminescence decay curve of purified CdSe nanocrystals mixed with Cd(FA)₂. (e) Luminescence decay curve of purified CdSe nanocrystals mixed with TBP. (f) Luminescence decay curve of purified CdSe nanocrystals mixed with TOPO. A red dashed line was added as the linear fitting curve for the first few data points in (d–f).

crystals. Instead, facets might be a critical parameter to be considered. For the first time, we observed the relationship between nanocrystal size and intrinsic lifetime for CdSe core nanocrystals with different crystal lattices. For a given internal and surface inorganic structure/stoichiometry, primary amine was identified as the “ideal” ligands for the excitons in CdSe core nanocrystals to be radiative decay with unity yield and in single channel. Such ideal CdSe core nanocrystals could be a set of standard samples for surface science and spectroscopy related to semiconductor nanocrystals, both experimentally and theoretically.

EXPERIMENTAL SECTION

Chemicals. Octylamine (98%), selenium powder (Se, 200mesh, 99.999%), and 1-octadecene (ODE, 90%) were purchased from Alfa-Aesar. Cadmium formate (Cd(FA)₂, 99.9%) and oleylamine (NH₂OL, C₁₈ content 70%) were purchased from Aldrich. Tributylphosphine (TBP) was purchased from Shanghai Titan Chem. All organic solvents were purchased from Sinopharm Reagents. All chemicals were used directly without any further purification. All CdSe core nanocrystals used here were synthesized and purified following published procedures.¹¹

All fatty amines, fatty acid, and fatty acid salts followed a systematic abbreviation.¹¹ Fatty amines shall be represented by NH₂ and the uppercase first letter and lowercase second letter of the common name. For instance, oleylamine shall be written as NH₂OL. For fatty acids and cadmium salts, H and Cd shall replace NH₂. For example,

stearic acid and cadmium oleate shall be represented as HSt and Cd(OL)₂, respectively. Apparently, this system is consistent with the common abbreviation for acetic acid and its salts.

Typical Procedure for Surface Treatment. Purified CdSe nanocrystals (1.0×10^{-7} mol) were mixed with 1 mL NH₂OL, 3 mL ODE, and 0.1 mL 0.1 M Se suspension. The mixture was degassed with argon for 10 min and heated to 140 °C. After heating at 140 °C for 10 min, another 0.1 mL Se suspension (0.1 M) was added into the flask. This process was repeated 2 or 3 times until the CdSe nanocrystals were fully treated. Judgment of fully treated was empirical. For example, for ~4 nm CdSe nanocrystals, the last Se treatment should shift the UV peak position for no more than 2 nm. After the Se treatment, 0.2 mL TBP was added at 140 °C, and temperature was raised to 220 °C. After cooling to 30 °C, 0.4–0.5 mL 0.1 M cadmium formate was added dropwise into the solution. If cadmium formate was added at 100 °C, only 0.01–0.015 mL of 0.1 M cadmium formate solution was sufficient.

Optical Measurements. UV–vis absorption spectra were measured on an Analytik Jena S600 UV–vis spectrophotometer. The PL spectra were recorded by an Edinburgh Instruments FLS920 spectrometer. The absolute PL QY measurements were carried out on an integrating sphere (Ocean Optics FOIS-1) coupled with a QE65000 spectrometer. For each nanocrystal sample, multiple measurements were performed with solutions in a series of concentrations. PL lifetime measurements were carried on a transient fluorescence spectrometer (Edinburgh Instruments FLS920), and the samples were excited by a 405 nm picosecond pulsed laser at a repetition frequency of 2 MHz. The peak photon counts were always fixed as 5000, and the optical density at the lowest-energy absorption peak of the nanocrystals kept below 0.2. For all plots, the y-axis was in logarithm.

X-ray Powder Diffraction (XRD). XRD measurements were carried on a Rigaku Ultimate-IV X-ray diffractometer operated at 40 kV/30 mA with Cu K α line ($\lambda = 1.5418$ Å). Nanocrystals powder samples placed onto glass substrates were prepared by the standard precipitation procedure with hexanes as the solvent and acetone as the precipitation reagent.

AUTHOR INFORMATION

Corresponding Author

*xpeng@zju.edu.cn

Notes

The authors declare no competing financial interest.

ACKNOWLEDGMENTS

This work was supported by the National Natural Science Foundation of China (21233005 and 91433204).

REFERENCES

- (1) Murray, C. B.; Kagan, C. R.; Bawendi, M. G. *Annu. Rev. Mater. Sci.* **2000**, *30*, 545.
- (2) Peng, X. G. *Nano Res.* **2009**, *2*, 425.
- (3) Zherebetskyy, D.; Scheele, M.; Zhang, Y. J.; Bronstein, N.; Thompson, C.; Britt, D.; Salmeron, M.; Alivisatos, P.; Wang, L. W. *Science* **2014**, *344*, 1380.
- (4) Jasieniak, J.; Mulvaney, P. *J. Am. Chem. Soc.* **2007**, *129*, 2841.
- (5) Li, J. J.; Wang, Y. A.; Guo, W. Z.; Keay, J. C.; Mishima, T. D.; Johnson, M. B.; Peng, X. G. *J. Am. Chem. Soc.* **2003**, *125*, 12567.
- (6) Wei, H. H.; Evans, C. M.; Swartz, B. D.; Neukirch, A. J.; Young, J.; Prezhdo, O. V.; Krauss, T. D. *Nano Lett.* **2012**, *12*, 4465.
- (7) Omogo, B.; Aldana, J. F.; Heyes, C. D. *J. Phys. Chem. C* **2013**, *117*, 2317.
- (8) Subila, K. B.; Kumar, G. K.; Shivaprasad, S. M.; Thomas, K. G. *J. Phys. Chem. Lett.* **2013**, *4*, 2774.
- (9) Qu, L. H.; Peng, X. G. *J. Am. Chem. Soc.* **2002**, *124*, 2049.
- (10) Pu, C. D.; Zhou, J. H.; Lai, R. C.; Niu, Y.; Nan, W. N.; Peng, X. G. *Nano Res.* **2013**, *6*, 652.
- (11) Gao, Y.; Peng, X. G. *J. Am. Chem. Soc.* **2014**, *136*, 6724.

- (12) Bawendi, M. G.; Carroll, P. J.; Wilson, W. L.; Brus, L. E. *J. Chem. Phys.* **1992**, *96*, 946.
- (13) Kim, S.; Bawendi, M. G. *J. Am. Chem. Soc.* **2003**, *125*, 14652.
- (14) Nan, W. N.; Niu, Y. A.; Qin, H. Y.; Cui, F.; Yang, Y.; Lai, R. C.; Lin, W. Z.; Peng, X. G. *J. Am. Chem. Soc.* **2012**, *134*, 19685.
- (15) Lakowicz, J. R. *Principles of fluorescence spectroscopy*, 3rd ed.; Springer: New York, 2006.
- (16) van Driel, A. F.; Allan, G.; Delerue, C.; Lodahl, P.; Vos, W. L.; Vanmaekelbergh, D. *Phys. Rev. Lett.* **2005**, *95*, 236804.
- (17) Efros, A. L.; Rosen, M.; Kuno, M.; Nirmal, M.; Norris, D. J.; Bawendi, M. *Phys. Rev. B* **1996**, *54*, 4843.
- (18) Califano, M.; Franceschetti, A.; Zunger, A. *Phys. Rev. B* **2007**, *75*, 115401.
- (19) Norris, D. J.; Efros, A. L.; Rosen, M.; Bawendi, M. G. *Phys. Rev. B* **1996**, *53*, 16347.
- (20) Nirmal, M.; Norris, D. J.; Kuno, M.; Bawendi, M. G.; Efros, A. L.; Rosen, M. *Phys. Rev. Lett.* **1995**, *75*, 3728.
- (21) Biadala, L.; Louyer, Y.; Tamarat, P.; Lounis, B. *Phys. Rev. Lett.* **2009**, *103*.
- (22) Leung, K.; Whaley, K. B. *J. Chem. Phys.* **1999**, *110*, 11012.
- (23) Ji, X. H.; Copenhaver, D.; Sichmeller, C.; Peng, X. G. *J. Am. Chem. Soc.* **2008**, *130*, 5726.
- (24) Talapin, D. V.; Rogach, A. L.; Shevchenko, E. V.; Kornowski, A.; Haase, M.; Weller, H. *J. Am. Chem. Soc.* **2002**, *124*, 5782.